Analysis of Silicon Nanocrystals in Silicon-rich SiO_2 Synthesized by CO_2 Laser Annealing

Chun-Jung Lin[1], Gong-Ru Lin[1]*, Yu-Lun Chueh[2], Li-Jen Chou[2],
[1]Department of Photonics & Institute of Electro-Optical Engineering,
National Chiao Tung University,
1001, Ta Hsueh Rd., Hsinchu, Taiwan 300, R. O. C.
[2]Department of Materials Science and Engineering
National Tsing Hua University
101, Sec. 2 Kuang Fu Rd., Hsinchu, Taiwan 300, R. O. C.
*Corresponding author. Phone: 886-3-5712121 ext. 56376; Fax: 886-3-5716631; E-mail: grlin@faculty.nctu.edu.tw

ABSTRACT

The localized synthesis of 4.2-5.6 nm-Si nanocrystals (nc-Si) in Si-rich SiO_2 (SRSO) by CO_2 laser annealing at laser intensity of below ablation-threshold (6 kW/cm^2) is demonstrated. Since the SRSO exhibits a high absorption coefficient of up to 0.102 cm^{-1} at wavelength of 10.6 μm, a direct-writing CO_2 laser annealing system with focusing spot size of 0.2 mm^2 is used to locally anneal the SRSO and precipitate the nc-Si. A thermophysical model reveals that the surface temperature of SRSO ranging from 130°C to 3350°C is achieved by varying the laser power densities from 1.5 to 13.5 kW/cm^2. The CO_2 laser-ablation-threshold power density is about 6 kW/cm^2, corresponding to the optimized annealing temperature 1285°C at the ablation threshold. The CO_2 laser annealing is capable of the precise control on power density and spot size, which benefits from the in-situ and localized annealing temperature control of SRSO film, and also prevents from the eternal damage of the other electronic devices nearby the annealing site. The nc-Si dependent photoluminescence (PL) were observed at 806 nm or longer, whereas the laser-ablation damaged SRSO film exhibits significant blue PL at 410 nm due to the oxygen-related structural defects. The refractive index of the laser-treated SRSO film is increasing from 1.57 to 2.31 as the laser intensity increases from 1.5 to 6.0 kW/cm^2 which is mainly attributed to the increasing density of nc-Si embedded in SRSO. High resolution transmission electron microscopy (HRTEM) analysis reveals that the average size of nc-Si embedded in SRSO film is about 5.3 nm, which correlates well with the theoretical prediction of a corresponding PL at 806 nm. The HRTEM estimated square density of the nc-Si in SRSO film under the laser intensity of 6 kW/cm^2 is about 10^{18} cm^{-3}.

Keywords: CO_2 laser annealing, Photoluminescence, Silicon nanocrystal, Silicon-rich silicon dioxide, HRTEM.

1. INTRODUCTION

Silicon-rich silicon oxide (SRSO) layer with buried Si nanocrystals (nc-Si) has emerged as a near-infrared light-emitting materials for next-generation all-Si based optoelectronic integrated circuits.[1] Previously, several technologies have been proposed for fabricating the SRSO material, such as electron-beam evaporation,[2] Si-ion-implantation,[3] plasma-enhanced chemical vapor deposition[4] (PECVD) and RF-magnetron sputtering.[5] Ye *et al*.[2] have reported that a thin a-Si layer is deposited by e-beam evaporation, followed by simultaneous crystallization and oxidation at 800°C for 20 min in a 3:1 dry N_2 and O_2 mixture at a total pressure of one atmosphere, which results in the nanocrystallite Si with the diameter of about 200 nm. Pérez-Rodríguez *et al*.[3] have synthesized the SRSO film by implanting the 150 keV Si^+ ions into the 400 nm-thick SiO_2 layer, and they have released the nc-Si with the diameter of 1.4 nm after samples were annealed under N_2 atmosphere at 1100°C. Pacifici *et al*.[4] reported the structural and near-infrared-region optical properties of Si nanocrystals, with the diameters from 1.0 nm to 2.1 nm, formed by high temperature annealing (1000~1300°C) of SRSO thin film produced by plasma enhanced chemical vapor deposition. Toshikiyo *et al*.[5] have demonstrated SRSO films deposited by using a multi-target sputtering apparatus. After the growth of microcavity structures, the multi-layer structure was annealed in an N_2 gas atmosphere for 30 min at 1100°C and the active layer was a SiO_2 thin film containing nc-Si. Typically, a high-temperature furnace annealing (over 1000°C) process is required to precipitate nc-Si in the SRSO layer. However, the typical thermal annealing is not a localized treatment and could seriously damage the nearby electronic ICs on the same wafer. Laser irradiation has recently been employed for precipitating localized nc-Si in the SRSO layer. Rossi *et al*.[6] showed that the laser re-crystallization was previously

Optoelectronic Materials and Devices for Optical Communications,
edited by Shinji Tsuji, Jens Buus, Yi Luo, Proc. of SPIE Vol. 6020,
602020, (2005) · 0277-786X/05/$15 · doi: 10.1117/12.636158

demonstrated by using a tightly focused continuous-wave Ar^+ laser (λ= 514.5 nm), which helps to synthesize the nc-Si in hydrogenated amorphous SiO_x (a-SiO_x:H). In another study, it was demonstrated that using a pulsed, frequency-tripled Nd:YAG laser (τ=8 ns, λ=355 nm) with intensity increasing from 30 to 360 mJ/cm^2, the size of the nc-Si in a-SiO_x:H (with oxygen concentrations between 10 and 30 at. %) can be enlarged from 20 to 200 nm.[7] Later on, Gallas *et al*.[8] reported that for a 248 nm-KrF pulsed excimer laser the threshold intensity is 85 mJ/cm^2 for annealing SiO_x without any ablation. Nonetheless, it is relatively difficult to precipitate nc-Si in SRSO at such a low intensity due to the negligibly small absorption coefficient of SiO_2 at such a wavelength (for example, $\alpha<1\times10^{-6}$ cm^{-1} at <532 nm).[9] In this case, insufficient energy is transformed into the heat for nc-Si precipitation since the surface temperature is directly proportional to the absorption coefficient. In this Letter, a CO_2 laser is employed as the annealing source for the synthesis of the nc-Si in PECVD-grown SRSO layers on quartz substrates since the SRSO layer exhibits an absorption coefficient as high as 1.2×10^3 cm^{-1} at the laser wavelength of 10.6 μm. The size and density of nc-Si embedded in the SRSO layer after CO_2 laser annealing are studied by high resolution transmission electron microscopy (HRTEM). The evolution of the blue and near-infrared photoluminescence (PL) spectra from laser-annealed SRSO layers is investigated. The analysis of the Rutherford Backscattering Spectrometry (RBS), transmission and reflection spectrum of the SRSO layer is performed. The surface temperature simulation using the thermo-physical model is also demonstrated.

2. EXPERIMENT SETUP

2.1 Sample preparation

The Si-rich SiO_x film was grown on the double-side polished quartz substrates by using a PECVD system at pressure of 120 mtorr a N_2O/SiH_4 fluence ratio of 6:1 under forward power of 45 W. The N_2O fluence was controlled at 120 sccm. The quartz substrate temperature was hold at 150^{o}C for 15 min to balance the substrate and chamber temperature before deposition. After deposition, a continuous-wave CO_2 laser (LTT Corp., ILS-II with a maximum power of 30 W) was used to perform the laser annealing process in atmosphere and the laser intensities are ranging from 1.5 to 13.5 kW/cm^2. The CO_2 laser annealing time was set as 1 ms. The laser spot of the CO_2 laser was focused within 0.2 mm^2 using a hemispherical lens, which can only be reduced to 130 μm^2 (limited by Rayleigh criterion, D = 1.22 λ/NA, where D is the diameter of the spot, λ is the wavelength of the light source, and NA is the neutral aperture).

2.2 The thermo-physical model and the temperature gradient around the annealed zone

The temperature around the annealed zone is determined using a previously developed model published by Shiu *et al.*,[10] in which the heat transport due to convection, thermal radiation and thermal expansion are all neglected. The absorbed energy per unit volume and per unit time of the sample illuminating by a Gaussian laser beam shape is described as $g_{Laser}(r,z)=P_0(1-R)I_r(r)I_z(z)$ where P_0 is the laser power, R is the surface reflectivity, (R=[(n-1)^2+k^2]/[(n+1)^2+k^2]), $I_r(r)$ is the radial intensity profile of the laser beam at the SRSO surface, r is the distance to the center of the laser focus spot, $I_z(z)$ is the axial intensity attenuation of the beam, and z is the depth from the surface. The real (n) and imaginary (k) parts of the refractive indices of the SRSO at 10.6 μm are approximately 2.224 and 0.102, respectively. The focusing lens imposes a Gaussian distribution such that $I_r(r)=\frac{2}{\pi w^2}\exp(\frac{-2r^2}{w^2})$ where w is the Gaussian beam radius. According to Bouguer's Law, $I_z(z)$ is given by $I_z(z)=\alpha\exp(-\alpha|z|)$, where $\alpha=4\pi k/\lambda$ denotes the optical absorption coefficient, and λ is the laser wavelength. As a result, the temperature $T(r, z)$ and peak temperature T_{peak} of the SRSO film can be expressed as the following equations:[10,11]

$$T(r,z)=\frac{g_{Laser}(r,z)\tau}{\rho C_p}=\frac{\alpha(1-R)}{\rho C_p}\times\frac{2P_0\tau}{\pi w^2}\times\exp(\frac{-2r^2}{w^2})\times\exp(-\alpha|z|), \quad (1)$$

$$T_{peak}(r)=\frac{\alpha(1-R)}{\rho C_p}\times\frac{2P_0\tau}{\pi w^2}\times\exp(\frac{-2r^2}{w^2}), \quad (2)$$

$$\frac{\partial T_{peak}(r)}{\partial r}=(\frac{-4r}{w^2})\frac{\alpha(1-R)}{\rho C_p}\times\frac{2P_0\tau}{\pi w^2}\times\exp(\frac{-2r^2}{w^2}), \qquad r>0 \quad (3)$$

By setting the optical absorption coefficient (α), the optical reflectivity (R), the Gaussian beam radius (w), the radial distance (r), the illumination time (τ), the density (ρ), and the specific heat (C_p) of the SRSO as 1209 cm^{-1}, 0.145, 370 μm, 21 μm, 1 ms, 2800 kg/m^3 and 1270 J/kg/K, respectively. Therefore, from the Eq. (2), the T_{peak} of the SRSO layer surface, which is proportional to the laser intensity (P_{laser}), can be predicted. As the P_{laser} is increased from 1.5 to 13.5 kW/cm^2, the peak surface temperature of the SRSO is predicted to increase from 130°C to 3350°C. For example, the SiO_x surface temperature profile around the annealed zone under illuminating with laser intensity of 6 kW/cm^2 is shown in Fig. 1. The surface temperature at the central part of a Gaussian-beam illuminated zone is about 1349°C. The temperature gradient around the annealed zone of the SiO_x film is plotted in Fig. 2. The laser annealing temperature is decreasing from 1350°C at surface to 1295°C at the SRSO/Si interface. Within an illuminating spot of 400μm diameter, the maximum temperature gradient is about 4.5 °C/μm.

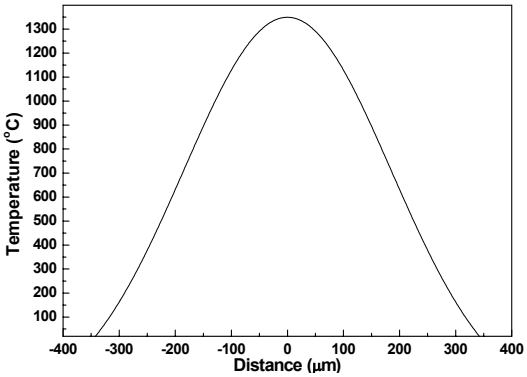

Fig. 1 Surface temperature of the annealing zone illuminated by CO_2 laser at 6 kW/cm^2

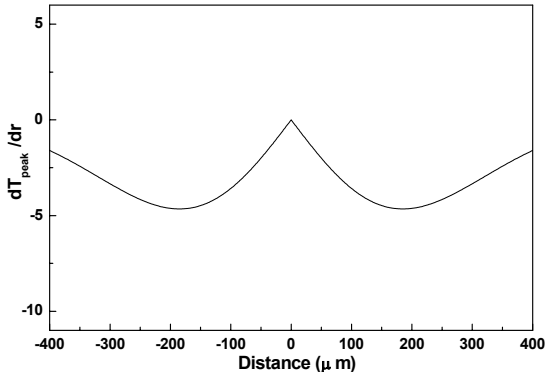

Fig. 2 The temperature gradient around the annealed zone.

2.3 The technique employed for optical properties, structure properties and refractive index measurements

The ablation thickness of the SRSO layer was measured by the α-step profiler or the atomic force microscope with a depth resolution of 1 nm. The PL of laser-treated SRSO was excited by a He-Cd laser with an intensity of 5 W/cm^2 at 325 nm and was analyzed by a monochromator (Jobin Yvon, TRIAX-320) and a photomultiplier (Hamamatsu, R928). The wavelength accuracy of the measurement system was confirmed by using an 850-nm laser diode. An HRTEM (JEOL, 4000EX TEM) with a point-to-point resolution of 0.17 nm was used to characterize the orientation, the lattice constant, the size, and the density of the precipitated nc-Si in the SRSO layer. RBS measurement at detecting angle of 170° under 2MeV He^+-ion bombardment is used to analyze the composition of Si in the SRSO layer.

A commercial n&k analyzer (n&k Technique Inc., 1700) for measuring the refractive index of the Si-rich SiO_x film was employed, which consists of a broadband light source with wavelength ranging from 190 nm to 1000 nm. The nondestructive n&k analyzer distinguishes signal with an excellent signal-to-noise ratio over the entire deep-UV to near-IR regime. By using the n&k analyzer, the data such as film thickness, bandgap energy, and the spectra for of refractive index (n) and extinction coefficient (k) can be extracted. The n&k method is strongly correlated with the Kramers–Kronig relation,[12–14] which is used to extract the necessary intrinsic quantities from the deconvoluted extrinsic quantities. The n&k analysis employs the Forouhi–Bloomer (FB) dispersion equations deduced by Forouhi *et al.*[12-14],

$$k(E) = \sum_{i=1}^{q} \frac{A_i (E - E_g)^2}{E^2 + B_i E + C_i} \tag{4}$$

$$n(E) = n(\infty) + \sum_{i=1}^{q} \frac{B_{oi} E + C_{oi}}{E^2 + B_i E + C_i} \tag{5}$$

The aforementioned equations describe the index of refraction *n(E)* and the extinction coefficient *k(E)*, where E_g represents the bandgap energy defined at absolute minimum of k(E), and the parameters of A_i, B_i and C_i are the fitting parameters dependent with the electronic configuration of the material.[12–14] The quantities of B_{oi} and C_{oi} are correlated with A_i, B_i, C_i. Each term in the summation is contributed either by a peak or by a shoulder of the spectra, and the number of terms equals to the number of discernible spectral peaks and shoulders.

3. RESULTS AND DISCUSSION

3.1 Structure Analysis

The output power of the CO_2 laser can be controlled by biasing the input current of the CO_2 laser. The precise control on the output power of CO_2 laser results in a fine adjustment of laser annealing temperatures on the SRSO film. The CO_2 laser annealing reduces the annealing time for precipitating nc-Si to 1 ms, which is much shorter than that required in a furnace-annealing process.[3] The other advantage of the CO_2 laser annealing is its localized treatment. The CO_2 laser beam can strongly focused into a spot size of ~10 μm, which can be position-controlled by using a programmable X-Y translation stage. Therefore, such a CO_2 laser based rapid-thermal-annealing process is capable of in-situ and localized temperature control. As a result, the CO_2 laser illuminated region of SRSO films turns from light-yellow to dark-yellow after annealing at laser intensities increasing from 3 to 13.5 kW/cm^2. (See Fig. 3) The change in color of the SRSO film is attributed to the variation of both the absorption coefficient and due to the precipitation of nc-Si embedded in the SRSO film.

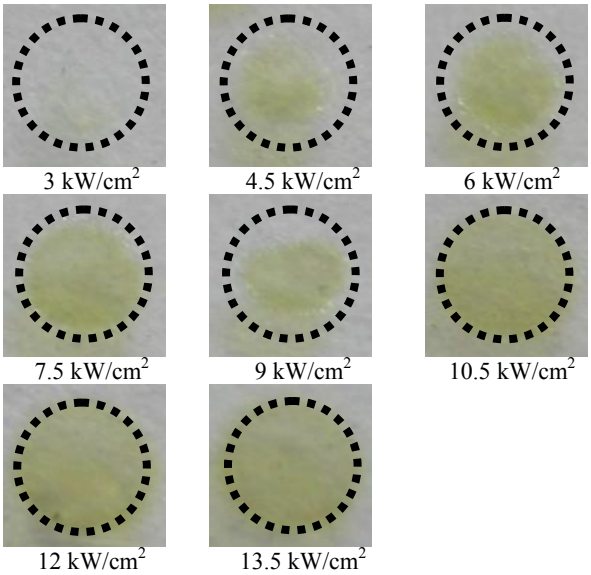

Fig. 3 Far-field patterns of SRSO films after CO_2 laser annealing at laser intensities from 3 to 13.5 kW/cm^2.

The composition of the SRSO film has also been analyzed by using RBS measurement, which bombards the SRSO film with 2MeV He^+-ions and picks up the backscattering signal at an angle of 170^o. The composition of the SRSO film was analyzed using commercial software "Genplot". The RBS spectrum of SRSO film indicates clear signals of Si and oxygen at 1.147 MeV and 742.0 keV, respectively, as shown in Fig. 4. It reveals that the thickness of the as-deposited SRSO film is about 280 nm, which is in good agreement with that measured by a surface profiler. The calculated ratio of O/Si in the SRSO film is 1.25, corresponding to a total Si concentration of about 44.44 atomic %. That is, the as-deposited SRSO film is $SiO_{1.25}$. Previously, a similar PL result attributed to the nc-Si in SiO_x film with 39 atomic % of Si after annealed at 1250^{o}C for 1 h was reported.[15] The existence and the size distribution of nc-Si embedded in the SRSO film, which was annealed at the CO_2 laser intensity of 6 kW/cm^2 is confirmed by the plan-view (see Fig. 5) HRTEM picture. The HRTEM pictures reveal the distribution of nc-Si diameter within 4.2-5.6 nm (average diameter of 5.3 nm), shown in the left picture of Fig. 5. The lattice space and orientation of the nc-Si are determined as 0.3 nm and (111), respectively. (See the right picture of Fig. 5)

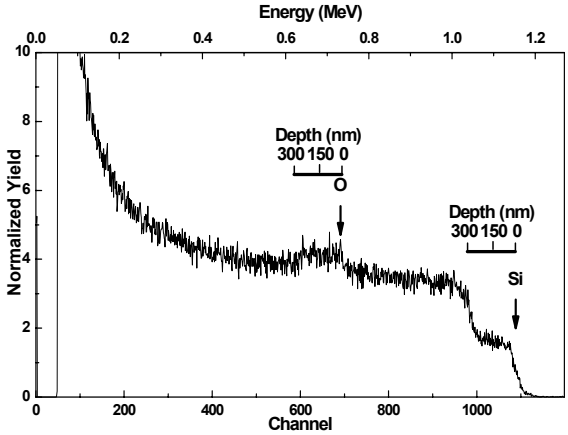

Fig. 4 The RBS spectrum of the Si-rich SiO_x film.

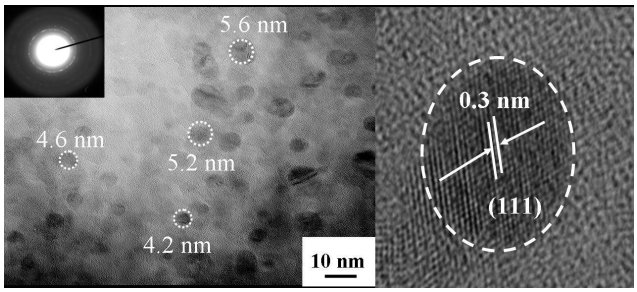

Fig. 5 Plan-view high-resolution transmission electron microscopy pictures.

3.2 Density of Si nanocrystals

The surface density of the nc-Si buried in the SRSO film annealed at the CO_2 laser intensity of 6 kW/cm^2 was estimated about 2.59×10^{13} cm^{-2}, which was calculated from the planar photograph of the SiO_x film taken by the HRTEM. After annealing by a CO_2 laser at the laser intensity of 6 kW/cm^2, the thickness of the sample was shrunk 240 nm as determined by cross-sectional HRTEM. The volume density ρ of the nc-Si buried in the CO_2 laser-annealed sample is about 1.08×10^{18} cm^{-3} as calculated by $\rho = (\phi / thickness) = (2.59\times10^{13}\ cm^{-2} / 240\,nm)$.

Since the Si exhibits a diamond lattice structure that consists of eight atoms in a unit cell. Taking the Si lattice constant of 0.543 nm, the number of Si atoms per cubic centimeter of $8/a^3 = 8/(5.43\times10^{-8})^3 = 5\times10^{-22}$ atoms/cm^3 can be obtained. The estimated average diameter and volume of the buried nc-Si are about 5.3 nm and 7.79×10^{-20} cm^3, respectively. In this case, such an nc-Si is constructed by 3897 Si atoms (N=7.79×10^{-20} cm^3 × 5.43×10^{-22} atoms/cm^3=3897 atoms). Since the density of the PECVD-grown SiO2 is 1.4 g/cm^3. Therefore, the number of Si atom per cubic centimeter in the PECVD-grown SiO_2 is about 1.4×10^{22} atoms/cm^3, as calculated by

$$\frac{6.0221\times10^{23}\,atoms/mol\times1.4\,g/cm^3}{60\,g/mol} = 1.40515666\times10^{22}\ atoms/cm^3 \quad (6)$$

The atomic mass of the $SiO_{1.25}$ becomes 48 amu, and the evaluated density of $SiO_{1.25}$ is 1.95 g/cm^3, which is linearly interpolated the density of SiO material (D_{SiO} = 2.13 g/cm^3). Therefore, the number of Si atom per cubic centimeter of the PECVD-grown $SiO_{1.25}$ film is calculated as 2.45×10^{22} atoms/cm^3.

$$\frac{6.0221\times10^{23}\ atoms/mol\times1.95\ g/cm^3}{48\,r/mol} = 2.44647812\times10^{22}\ atoms/cm^3 \quad (7)$$

Consequently, the number of the 11.11 atomic % of excess Si atoms buried in the $SiO_{1.25}$ film in our experiment is about 1.04132146×10^{22} atoms/cm^3.

$$N_{Si/SiO_2} - N_{Si/SiO_2} = (2.44647812 - 1.40515666)\times10^{22}\ atoms/cm^3 \quad (8)$$

By using this value, the number of the nc-Si buried in $SiO_{1.25}$ film is calculated as about 2.67×10^{18} cm^{-3} using $N_{nc\text{-}Si}$ = (1.041324146×10^{21} atoms/cm^3) / (3897 atoms per one nc-Si). The plan-view HRTEM-estimated maximum volume density of the nc-Si in the SRSO layer annealed at 6.0 kW/cm^2 is about 1.08×10^{18} cm^{-3}, which is corroborated with the theoretically estimated density of 2.67×10^{18} cm^{-3} under the assumption that an nc-Si with average diameter of 5.3 nm contains nearly 3900 Si atoms.

3.3 CO2 Laser Ablation Effect

The ablation depth of the SRSO layer was measured as a function of the laser intensity (P_{laser}) ranging from 1.5 to 13.5 kW/cm^2, as shown in Fig. 6.

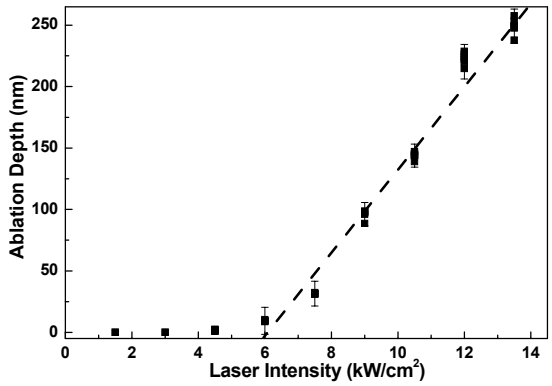

Fig. 6 CO_2 laser ablated SRSO thickness as a function of the laser intensity

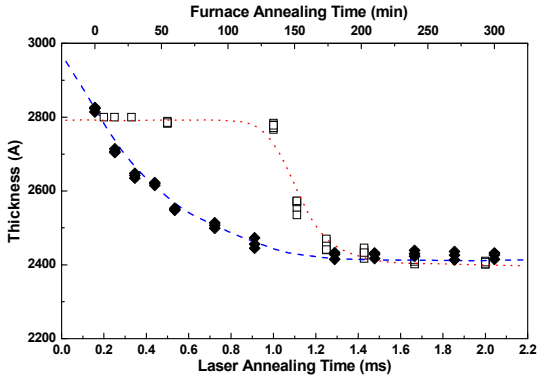

Fig. 7 Thickness of the SRSO film as a function of the laser or furnace annealing time.

Note that since the as-grown SRSO layer contains high concentration of hydrogen, the pre-annealing is used to obtain a hydrogen-free, compact SRSO layer owing to the loss of hydrogen during the annealing. To distinguish the shrinkage in SRSO film thickness either by CO_2 laser annealing induced de-hydrogenation or by CO_2 laser ablation process, the SRSO sample was first de-hydrogenated by annealing either in a furnace at 1100°C or with a CO_2 laser at intensity of 4 kW/cm^2 (well below ablation threshold). The thicknesses of the annealed SRSO films are plotted as a function of annealing time, as shown in Fig. 7. The de-hydrogenating process is finished after furnace annealing at 1100°C for three hrs, while the thickness of the annealed SRSO film reduces from 281 nm to 242 nm. Similar result is also observed in the CO_2 laser annealed SRSO sample after illuminating for 1.4 ms or longer. The shrinking depth of the PECVD-grown SRSO film during annealing is about 38-39 nm. Since a PECVD-grown SRSO film contains high concentrations of hydrogen, the loss of hydrogen during annealing is attributed to the compaction of the SRSO film. Afterwards, the CO_2 laser ablation experiment was performed using the de-hydrogenated SRSO film with thickness of about 240 nm. This is done by illuminating the SRSO sample in atmosphere with a CO_2 laser at different intensities (ranging from 1.5 to 13.5 kW/cm^2). The ablation depth of the SRSO film was measured as a function of laser intensities, as shown in Fig. 6. A linear ablation slope of 29 nm/(kW/cm^2) was observed at $P_{laser} > 6$ kW/cm^2.
Moreover, the refractive index of the laser-annealed SRSO layer at the wavelength of 633 nm measured by a commercial n&k analyzer (n&k Technique Inc., 1700) is greatly increased from 1.57 to 2.31 as P_{laser} is increased from 1.5 to 6.0 kW/cm^2 (see the inset of Fig. 8). At a surface temperature below 600°C (or P_{laser} <3 kW/cm^2), the change in refractive index of the laser-annealed SRSO layer is less than 0.6 % since the precipitation of nc-Si has not been initiated yet. The refractive index of SRSO layer increases from 1.93 to 2.31 as the annealing temperature increases from 900 to 1300°C. That is, the nc-Si precipitation becomes more pronounced at larger CO_2 laser intensity. In previous studies, Prakash *et al.*[16] have measured refractive indices of 1100°C annealed PECVD-grown SRSO films with total Si concentrations of 39 atomic %, 42 atomic % and 46 atomic % are 1.84, 1.93 and 2.15, respectively. Later on, Khriachtchev *et al.*[17] have also reported that the refractive index increases with the excess Si concentration, in which the refractive indices of the 1150°C annealed Si-rich SiO_x samples with x = 1.85, 1.57 and 1.45 are 1.65, 1.8 and 1.9, respectively. Moreover, Naciri *et al.*[18] also observed that the refractive index of a SiO_2 film can be increased up to 2.3 at 633 nm after implanting with Si ions at a fluence of 8×10^{18} cm^{-2} at substrate temperature of 500°C and annealing at 1100°C for 2 hrs. All of the aforementioned results strongly corroborate the refractive index of a thermally annealed SRSO film can be much higher that that of a standard SiO_2 film (n = 1.455 at 633 nm), which is directly attributed to the precipitated nc-Si in the SRSO film. According to previous studies,[16-18] it can be confirmed that the refractive index of annealed SRSO increases as the excess Si precipitates. The density of the nc-Si film significantly enlarges as the excess Si concentration of the SRSO film increases.

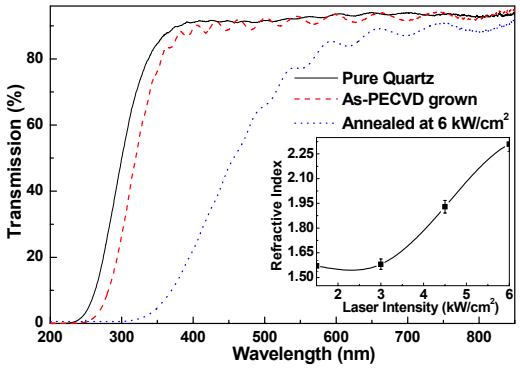

Fig. 8 Transmission spectrum of pure quartz, as-PECVD grown sample and SRSO sample annealed at laser intensity of 6 kW/cm^2. Inset: Refractive index of SRSO film after CO_2 laser annealing at laser intensities from 1.5 to 6 kW/cm^2.

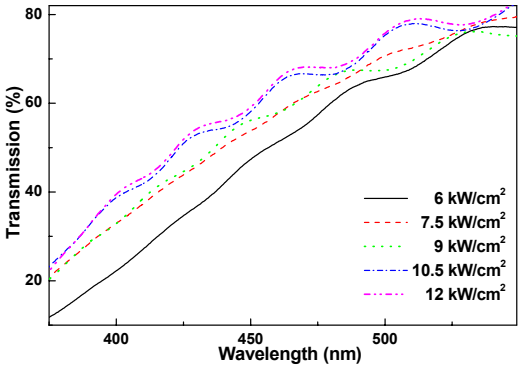

Fig. 9 Transmission spectra of SRSO samples annealed at laser intensities from 6 to 12 kW/cm^2.

3.4 Transmission and Reflection Spectroscopy

The transmission spectrum of the as-PECVD grown sample shows a redshift phenomenon in comparison with that of the pure quartz, as shown in Fig. 8, which is attributed to the 11.11 atomic % of excess Si atoms buried in the $SiO_{1.25}$ film. The interference fringes from 350 nm to 750 nm demonstrate the thickness and the different refractive indexes between the SRSO film and pure quartz. After the CO_2 laser annealing at the laser intensity of 6 kW/cm^2, the laser-annealed SRSO sample shows a stronger absorption between 300 nm and 750 nm than that of the as-PECVD grown sample and pure quartz. The obviously redshift transmission spectrum from the laser annealed SRSO sample is attributed to the precipitation of nc-Si embedded in the SRSO layer. Moreover, the dark far-field pattern and the higher refractive index, which is more close to the refractive index 3.5 of Si, of the CO_2 laser annealed SRSO sample at the intensity of 6 kW/cm^2 are also corresponded to the redshift transmission spectrum. The transmission spectra of the SRSO samples annealed at the laser intensities from 6 to 12 kW/cm^2 illustrate a blueshift phenomenon from 456.6 nm to 422.4 nm at the transmission of 50 %. (See Fig. 9) The increasing transmission at the wavelength of 410 nm is also corresponded to the decreasing depth of the SRSO layer. Although a linear ablation slope of 29 nm/(kW/cm^2) was observed at P_{laser} > 6 kW/cm^2, the SRSO layer will be ablated and become thinner, which results in that the transmission at a constant wavelength will be saturated.

The refractive index of the CO_2 laser annealed SRSO film dramatically decreases to 1.42 or less at P_{laser} higher than the ablation threshold of 6 kW/cm^2. This is due to the damage of the SRSO film under the laser ablation process, which generates numerous structural defects and fails to precipitate high-density nc-Si within the annealing duration. When annealing at P_{laser}>6 kW/cm^2, the laser intensity reaches the optical damage threshold of the SRSO film, which seriously generates the oxygen-related defects due to the destroy of the structure, and reduces the excess Si density through strong oxidation process. This eventually leads to an amorphous SiO_x film with few nc-Si. As an evidence, the nc-Si related PL blue-shifts from 806 nm to 763 nm with a decreasing signal amplitude. In principle, the linear proportionality between the PL intensity and the nc-Si density can be referred to the equation of $I \propto \varphi \sigma N / \tau$. Another strong evidence for the structural damage as well as the decreasing refractive index is the presence of blue PL in the laser ablated SRSO film, which is directly attributed to the oxygen-related NOV and weak-bonding defects. These defects usually appear in the strongly damaged or disordered SiO_x film. In our case, the 410-nm PL is mainly contributed by the weak-oxygen-bond defect. Such defects are generated by the bonding of oxygen interstitials in the damaged SRSO structure. Therefore, the laser ablated SRSO structure becomes amorphous with its refractive index close to the amorphous SiO_x film.

3.5 Photoluminescent Spectra of SRSO layers after CO_2 laser annealing

After CO_2 laser annealing at laser intensity of 1.5 kW/cm^2, a broadband blue-green PL contributed by the radiative defects such as E'_δ centers[19] (a precursor of nc-Si) at 520 nm and the neutral oxygen vacancies centers[20] (NOV) center at 455 nm are observed (see Fig. 10 (a)). The PL response of the laser-annealed SRSO layer is similar to that of furnace-annealed SRSO layer and is enhanced due to the activation of NOV and E'_δ defects at the high laser intensity of

3 kW/cm^2. Near the central region of the annealing spot, the precipitation of small-size nc-Si (with a size of 0.8-1 nm) from E'$_\delta$ defects is initialized as the PL has further red-shifted to 600-620 nm at P_{laser} = 4.5 kW/cm^2 (or a corresponding surface temperature of 1100^{o}C). A significant PL feature at 806 nm with spectral width of 106 nm is observed at laser intensity of 6 kW/cm^2, as shown in Fig. 10 (d).

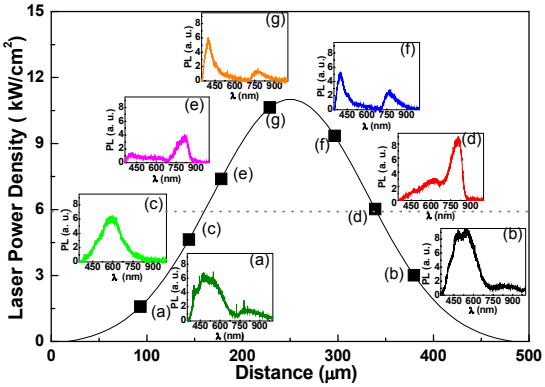

Fig. 10 PL spectra of CO_2 laser annealed SiO_x at different site of the annealed spot area. The CO_2 laser intensities are (a) 1.5 (b) 3 (c) 4.5 (d) 6 (e) 7.5 (f) 9 (g)10.5 kW/cm^2.

The maximum PL peak wavelength is observed at 825 nm at P_{laser} = 7.5 kW/cm^2. Nonetheless, the density of nc-Si in SiO_x also decreases at higher annealing laser power densities as the PL intensity at corresponding wavelength is greatly attenuated by an order of magnitude. To prove the strong correlation between the 806-nm PL and the nc-Si in laser-annealed SRSO layer, the PL and HRTEM of the as-grown and the annealed areas on the same SRSO sample were compared. In our case, no PL and no nc-Si precipitation was detected in the as-grown area. The corresponding temperature on the SiO_x surface is up to 1902 ^{o}C as P_{laser} becomes >7.5 kW/cm^2, which has already exceeded over the melting temperature of fused silica. In addition, the laser ablation of SiO_x inevitably leads to an increasing of structural damage related PL at 410 nm by one order of magnitude, which originates from the weak-oxygen-bond defect (O-O)[19] generated by the damaged bonds of the SiO_2 matrix (see the inset (f)-(g) of Fig. 10).

In addition, a slight red-shift in the PL peak wavelength from 806 to 825 nm is found as the laser intensity increases further from 6 to 7.5 kW/cm^2, indicating that an increase in size of the nc-Si. This result is in good agreement with previous observations of a similar red shift of the peak wavelength from 700 to 950 nm due to an increase in thermal annealing temperature from 1100 to 1250^{o}C.[15] However, the continuously increased size of the residual Si nanocrystals (corresponding to a further red-shift in PL wavelength) accompanies the greatly reduced nc-Si density due to the ablation and precipitation effects. Consequently, the ablation of the SRSO layer occurring at such high laser intensity inevitably leads to PL feature at the wavelength of 410 nm due to structural damage. This also results in a concurrent decrease in the near-infrared PL intensity by an order of magnitude, whereas the intensity of blue PL at 410 nm varies oppositely. The 410-nm PL feature is attributed mainly to the O-O defect[21] generated by the bonding of oxygen interstitials in the structure-damaged SRSO layer under high-intensity annealing treatment. In fact, the 410-nm PL intensity is increased by a factor of 7 as the laser intensity increases from 7.5 to 11 kW/cm^2. The surface temperature of the SRSO layer can be as high as 1902^{o}C at P_{laser}>11 kW/cm^2, which exceeds the melting temperature of fused silica. The PL spectra detected at different annealing points across the entire CO_2 laser-annealed spot are shown in Fig. 10. The highest power of the CO_2 laser as well as the peak surface temperature on the SRSO layer are located in the center of the circular, Gaussian-distributed CO_2 laser beam spot. Peak wavelengths of PL ranging from 600 to 620 nm are observed and attributed to a lower annealing temperature within the outer area of the laser-annealed spot, resulting from a weaker nc-Si precipitating process. On the other hand, the PL peak wavelength at 806 nm is observed near the center of the illuminated laser spot. These results suggest that precise control over the intensity and spot size of the CO_2 laser can provide the advantage of *in-situ* temperature control in the localized laser-annealing process of the SRSO layers. Such control can also prevent permanent damage of the other electronic ICs near the annealing location. A laser beam shaper is mandatory, however, to flatten the Gaussian-distributed intensity profile within the focused beam spot for practical annealing applications.

4. CONCLUSION

In conclusion, the structural and optical properties of the PECVD-grown Si-rich SiO_x annealed film by CO_2 laser are primarily characterized by using PL, RBS, transmission spectrum and HRTEM in this work. The localized synthesis of nc-Si embedded in the PECVD-grown $SiO_{1.25}$ layer on quartz is proposed by using CO_2 laser annealing. These are obtained at just below ablation-threshold power density (6 kW/cm^2), which is at least 2 orders of magnitude smaller than that required for visible or UV lasers. A linear ablation slope of 29 nm/(kW/cm^2) was observed at $P_{laser} > 6$ kW/cm^2. The refractive index of the CO_2 laser annealed SRSO film varies from 1.57 to 2.31 as the P_{laser} increases from 1.5 to 6 kW/cm^2. At the $P_{laser} < 3$ kW/cm^2, the change in refractive index is less than 0.6 % since the precipitation of nc-Si has not yet been initiated. The refractive index of SiO_x reaches maximum as the surface temperature increases to 1285^{o}C, while the average diameter of nc-Si is also the largest. Annealing at higher power densities not only damages the SiO_x structure, but also constrains the precipitation and nc-Si and decreases the refractive index of the SiO_x. The peak temperature at the ablation threshold is about 1285^{o}C as estimated by using a thermophysical model. The evolution from blue-green to near-infrared PL emission versus laser intensity is investigated. Through PL spectrum analysis, contributions from Si-related defects, such as the weak oxygen bond, NOV, E'_δ defects, and nc-Si (790-806 nm) by laser annealing at different intensity are observed. The refractive index of laser-annealed SRSO layers at the wavelength of 633 nm can be as high as 2.31 after annealing at the laser intensity of 6.0 kW/cm^2. The change in structure and the precipitation of nc-Si in SRSO layers annealed under CO_2 laser irradiation are similar to those treated by a conventional thermal annealing process. HRTEM analysis reveals that when the average size of Si nanocrystals embedded in the SRSO layer is about 5.3 nm, the dispersion is about 4.2-5.6 nm. The volume density of the nc-Si in the SRSO layer annealed using the laser intensity of 6.0 kW/cm^2 is determined as 1.08×10^{18} cm^{-3}. The CO_2 laser annealing has the potential to achieve *in-situ* and localized temperature control on the synthesis of nc-Si in the SRSO layers without damaging the nearby devices.

ACKNOWLEDGEMENT

This work was supported in part by the National Science Council (NSC) of the Republic of China under grant NSC 93-2215-E-009-007 and NSC 94-2215-E-009-040.

REFERENCES

1. L. Pavesi, L. Dal Negro, C. Mazzoleni, G. Franzo, and F. Priolo, "Optical gain in silicon nanocrystals," *Nature (London)*, vol. 408, pp. 440-444, 2000.
2. Q. Ye, R. Tsu, and E. H. Nicollian, "Resonant tunneling via microcrystalline-silicon quantum confinement," Phys. Rev. B, vol. 44, pp. 1806-1811, 1991.
3. A. Pèrez-Rodrìguez, O. González-Varona, B. Garrido, P. Pellegrino, J. R. Morante, C. Bonafos, M. Carrada, and A. Claverie, "White luminescence from Si^+ and C^+ ion-implanted SiO_2 films," J. Appl. Phys., vol. 94, pp. 254-262, 2003.
4. D. Pacifici, E. C. Moreira, G. Franzo, V. Martorino, and F. Priolo, "Defect production and annealing in ion-irradiated Si nanocrystals," Phys. Rev. B, vol. 65, pp. 1441091-1-13, 2002.
5. K. Toshikiyoa, M. Fujiib, and S. Hayashia, "Enhanced optical properties of Si nanocrystals in planar microcavity," Phys. E, vol. 17, pp. 451-452, 2003.
6. M. C. Rossi, S. Salvatori, F. Galluzzi, and G. Conte, "Laser-induced nanocrystalline silicon formation in a-SiO matrices," Mater. Sci. Eng. B, vol. 69-70, pp. 299-302, 2000.
7. A. Janotta, Y. Dikce, M. Schmidt, C. Eisele, M. Stutzmann, M. Luysberg, and L. Houben, "Light-induced modification of a-SiOx II: Laser crystallization," J. Appl. Phys., vol. 95, pp. 4060-4068, 2004.
8. B. Gallas, C.-C. Kao, S. Fisson, G. Vuye, J. Rivory, Y. Bernard, and C. Belouet, "Laser annealing of SiOx thin films," Appl. Surf. Sci., vol. 185, pp. 317-320, 2002.
9. E. D. Palik, Handbook of Optical Constants of Solids, p. 762, Academic Press, Washington, 1985.
10. T. R. Shiu, C. P. Grigoropoulos, D. G. Cahill, and R. Greif, "Mechanism of bump formation on glass substrates during laser texturing," J. Appl. Phys., vol. 86, pp. 1311-1316, 1999.
11. J. Zhao, J. Sullivan, J. Zayac, and T. D. Bennett, "Structural modification of silica glass by laser scanning," J. Appl. Phys., vol. 95, pp. 5475-5482, 2004.
12. A. R. Forouhi and I. Bloomer, "Optical dispersion relations for amorphous semiconductors and amorphous dielectrics," Phys. Rev. B, vol. 34, pp. 7018-7026, 1986.
13. A. R. Forouhi and I. Bloomer, "Optical properties of crystalline semiconductors and dielectrics," Phys. Rev. B, vol. 38, pp. 1865-1874, 1988.

14. A. R. Forouhi and I. Bloomer, U.S. Patent No. 4,905,170.
15. F. Iacona, G. Franzo, E. C. Moreira, D. Pacifici, A. Irrera, and F. Priolo, "Luminescence properties of Si nanocrystals embedded in optical microcavities," Mater. Sci. Eng. C, vol. 19, pp. 377-381, 2002.
16. G. V. Prakash, M. Cazzanelli, Z. Gaburro, L. Pavesi, F. Iacona, G. Franzo, and F. Prilolo, "Linear and nonlinear optical properties of plasma-enhanced chemical-vapor deposition grown silicon nanocrystals," J. Modern Opt., vol. 49, pp. 719-730, 2002.
17. L. Khriachtchev, M. Rasanen, S. Novikov, and L. Pavesi, "Systematic correlation between Raman spectra, photoluminescence intensity, and absorption coefficient of silica layers containing Si nanocrystals," Appl. Phys. Lett., vol. 85, pp. 1511-1513, 2004.
18. A. E. Naciri, M. Mansour, L. Johann, J. J. Grob, and C. Eckert, "Correlation between silicon nanocrystalline size effect and spectroscopic ellipsometry responses," Thin Solid Films, vol. 455-456, pp. 486-490, 2004.
19. G.-R. Lin, C. J. Lin, and C. K. Lin, "Defect-enhanced photoconductive response of silicon-implanted borosilicate glass," Appl. Phys. Lett., vol. 85, pp. 935-937, 2004.
20. H. Nishikawa, R. Nakamura, and J. H. Stathis, "Oxygen-deficient centers and excess Si in buried oxide using photoluminescence spectroscopy," Phys. Rev. B, vol. 60, pp. 15910-15918, 1999.
21. J. C. Cheang-Wong, A. Oliver, J. Roiz, and J. M. Hernanaez, "Optical properties of Ir_2^+-implanted silica glass," Nucl. Instrum. Methods Phys. Res. B, vol. 175, pp. 490-494, 2001.